Proceedings of the 21st ICSMGE, Vienna, Austria, 14 – 19 June 2026. Pistrol, Adam & Schweiger (eds.)
Published by: ÖGG, Austrian Society for Geomechanics, Salzburg, Austria, ISBN 978-3-9503898-4-5
https://doi.org/10.53243/ICSMGE2026-634

Modelling Sand Boiling of a Detention Basin due to Internal Erosion During River Flooding

Kim Chan
Formerly GHD, Sydney, Australia, kimfchan@outlook.com

Bosco Poon
GHD, Sydney, Australia, bosco.poon@ghd.com

ABSTRACT: A detention basin was constructed below ground level adjacent to a river bridge abutment in northern NSW, Australia. The basin is located approximately 100 m landward of a levee designed for a 27-year return period flood. The subsurface profile comprises continuous sand and gravel layers up to 25 m thick, creating strong hydraulic connectivity between the river and the basin. During a 1-in-12-year flood, the river level rose to RL 6.5 m. Groundwater ingress and sand boiling were observed at the basin floor when its water level reached RL 1.5 m (i.e. about 0.5m above basin floor level). There was also observation of substantial loss of soil strength at the peripheral of the basin floor at the time of sand boiling. Shortly after sand boiling was detected, tension cracks and slope slippage were observed at the basin batter and the adjoining approach embankment of the highway. This paper presents a detailed numerical modelling study using transient flow analysis to investigate groundwater flow leading to sand boiling at the detention basin. A novel approach using a dummy material was employed to simulate seepage water entering the basin, addressing the limitation of the potential seepage face boundary, which assumes all water exiting the basin with zero pressure head. The paper also highlights the preferential seepage path through the gravel layer at depth rather than the overlying sand layers. This behavior is attributed to the contrast in hydraulic conductivity functions between the sand and gravel materials.

KEYWORDS: Sand boiling, permeability, flooding, groundwater flow, internal erosion, seepage analysis.

1 INTRODUCTION

Sand boiling and the associated internal backward erosion have long been recognized as an important consideration in the design of hydraulic structures such as embankment dams and levees. Many research studies have been carried out to understand the phenomenon and to develop analytical and design approaches (e.g. Bezuijen et al., 2019; Robbins et al., 2020; Schaefer et al., 2017; van Beek et al., 2010; Brennan, 2008; Pabst et al., 2008). However, sand boiling and backward erosion are rarely considered in the design of highway or railway projects.

This paper documents a case study where sand boiling occurred within a detention basin constructed to control stormwater runoff next to the approach embankment of a road bridge crossing a major river. Sand boiling was observed during two separate flood events in the river and led to slope instability of the approach embankment. Investigations and numerical back-analyses were conducted to assess the permeabilities of the sandy layers and to understand the likely mechanisms of sand boiling. The adopted remedial solution is also presented in the paper.

2 MECHANICS OF SAND BOILING

Sand boiling is the phenomenon when granular material is deposited on the ground surface concentrated around localised areas of vertical seepage paths. High hydraulic gradients across a low permeability layer below the ground surface are needed for sand boils to form. Sand boiling usually occurs downstream of embankments or levees during flood events and may lead to internal erosion piping in the foundation materials. The phenomenon of sand boiling and internal backward erosion has been discussed in detail in some publications, such as the technical report published by TAW, 1999 and a White Paper prepared by US Society on Dams, 2021.

The typical stages of sand boiling and backward erosion can be described as follows:

i. **Heaving of the covering layer on the downstream side** - A sufficiently high hydraulic gradient between the river level and the downstream groundwater level can result in elevated pore water pressures beneath the internal floor. The presence of a low-permeability layer above the internal floor can cause water pressure beneath the layer to approach or exceed the total stress imposed by its own weight. Under such conditions, effective stress is significantly reduced or becomes negative, resulting in upward displacement (heave) of the covering layer.
ii. **Rupture of the covering layer and creation of blow outs** – Rupturing in the covering layer can occur because of heaving. A channel can be created within the covering layer with the seepage water finding its way to the ground surface.
iii. **Erosion of the sand layer** – Sand particles can be transported from below the covering layer through the channels by the seepage water exiting the ground surface. The transported sand particles can make the water on the surface looks like 'boiling'.
iv. **Creation of pipes** – Without any appropriate remedial treatment, the channels can continue to grow, forming pipes by backward erosion.
v. **Collapse of the ground in surrounding area** – As a consequence of internal backward erosion, hollow spaces under the ground in the vicinity of the sand boils can form. When such hollow spaces are sufficiently large, subsidence of the ground can occur leading to cracking of the adjoining batter and slope instability.

3 PROJECT APPRAISAL AND DETAILS OF DETENION BASIN

A new bridge crossing over a major river at northern New South Wales, Australia was opened to the public in December 2019. On the northern approach embankment, a pump station and detention basin were constructed close to the northern abutment. The river is some 150 m to the south of the detention basin. The main purpose of the detention basin was to act as a storage facility to provide flow control through attenuation of stormwater runoff from the nearby town. A levee was also constructed along the riverbank to prevent water from flooding the nearby town center for a 1 in 27-year return period.

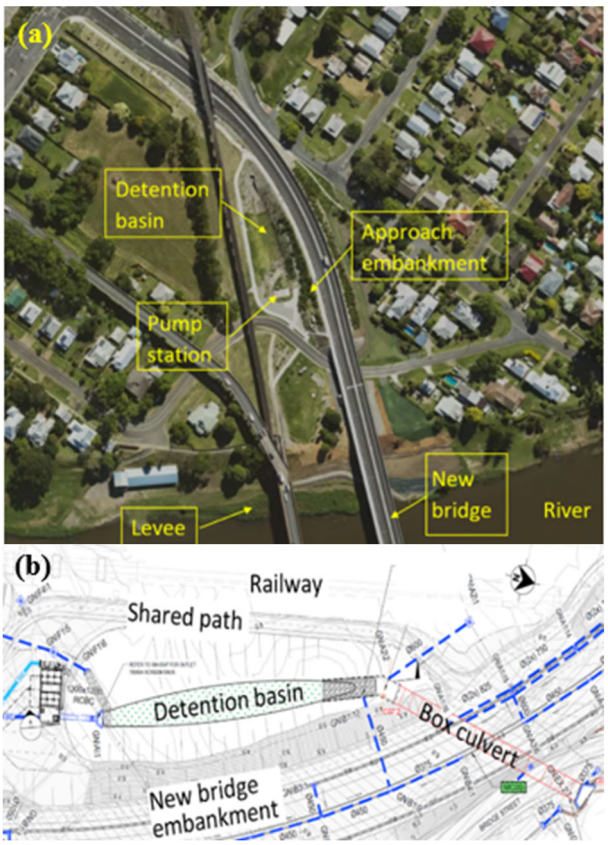

Figure 1. (a) Site setting showing the detention basin, the new bridge and the river and (b) general arrangement of detention basin, box culvert and new bridge embankment area.

The detention basin was designed to detain local stormwater runoff before discharging them to the river. At times when the water level in the basin reaches a certain level, the pumps will be activated, pumping local stormwater from within the basin to the river. The detention basin was an excavated area next to the toe of the western batter of the embankment. The invert level (at about RL 1.0 m or 3.9 m below the existing ground surface) was fixed based on the design hydraulic gradients of the drainage system.

The levee immediately next to the river was constructed with the top at about RL 7.5 m. Stormwater would discharge to the basin via a box culvert at the northern end of the basin. The stored water in the basin would then be pumped from the basin by the pumps located at the southern end of the basin to the river. Figure 1 shows the general arrangement and the northern box culvert relative to the river.

The basin floor was turfed and was normally dry when it was not used to store stormwater runoff. Sandy loam topsoil of about 0.3 m thickness was placed at the basin floor and batters to promote growing of the native grasses. Figure 2 shows the basin shortly after construction.


Figure 2. View of the basin shortly after construction

4 SEQUENCE OF EVENTS AND OBSERVATIONS

4.1 *Observations during the 2021 river flood*

On 24 March 2021, the water level in the river was recorded as high as RL 6.5 m, equivalent to approximately a 1 in 12-year flood event, but remaining below the crest of the levee without overtopping failure. At the same time, there was minimal raining within the region and flooding of the nearby town was not observed. Ingress of groundwater and sand boiling were observed at around 8:00 am (Figure 3a) when the water level in the basin reached around RL 1.5 m, i.e. about 0.5 m above basin floor level. There was also observation of substantial loss of soil strength at the peripheral of the basin floor. Tension cracks (Figure 3b) were observed at the basin batter at around 3:00 pm and movement was also observed at the top of the road embankment. Sand boiling was observed to gradually subside when the basin water level rose to approximately RL 2.5 m (Figure 3c).

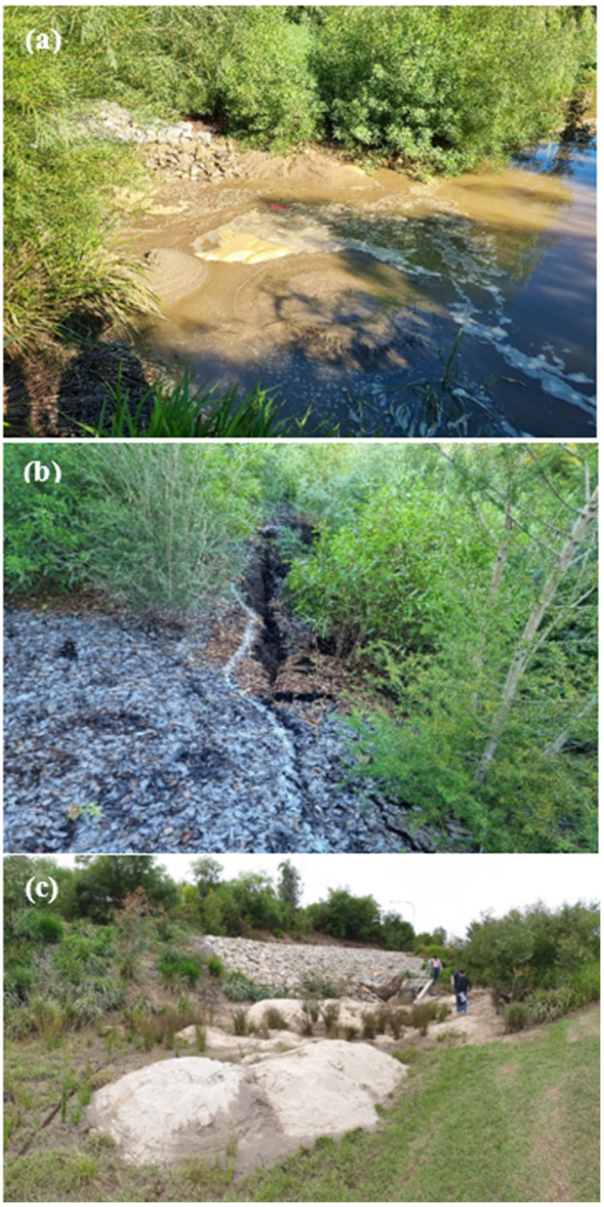

Figure 3. Observations of (a) water ingress and sand boiling in basin; (b) tension cracks on basin batter on 24 March 2021; and (c) sand deposited on basin floor after water subsided.

4.2 *Interim remedial measures*

Emergency measures were implemented at the time of sand boiling, which included allowing the basin water level to rise to RL 2.5 m and backfilling the slip zone of the basin batter with rock fill.

A couple of interim remedial options were also proposed after the flooding subsided as follows:

1. Placement of 0.5 m thick rockfill on the basin floor to counteract the uplift seepage pressure.
2. Installation of pressure relief wells to prevent sand boiling by reducing the seepage pressure beneath the basin floor.

Unfortunately, the proposed remedial measures were not implemented on site at that time.

4.3 *Observations during the 2022 river flood*

Another major flood event occurred on 28 February and 1 March, 2022 reaching a maximum level of RL 7.6 m for a few hours. Further sand boiling was observed resulting in significant erosion of the basin floor. Further embankment movement occurred with cracking at the embankment bench and tension crack opening up at top of the road embankment. Over 30 mm of lateral displacement at the road embankment was recorded. Settlement of the box culvert at the southern side of the basin of about 1 m was also detected. It was also observed that sand boiling appeared to have occurred at similar locations to those in March 2021.

5 GROUND MODEL

The existing ground profile prior to construction of the new bridge generally comprised Quaternary alluvium underlain by sedimentary rock. The Quaternary alluvium consisted of Holocene age deposits overlying Pleistocene age deposits. In the vicinity of the northern approach embankment, the Holocene alluvial profile can typically be described as loose sand layer of 4 to 5 m thickness. The underlying Pleistocene deposits can be described as medium dense sand layer of 7 to 12 m thickness. A 10 thick gravel layer exists between the sand layers and the underlying sedimentary bedrock.

A typical long section is shown in Figure 4 together with the approximate outline of the existing basin and notable water levels reported during the March 2021 flood event.

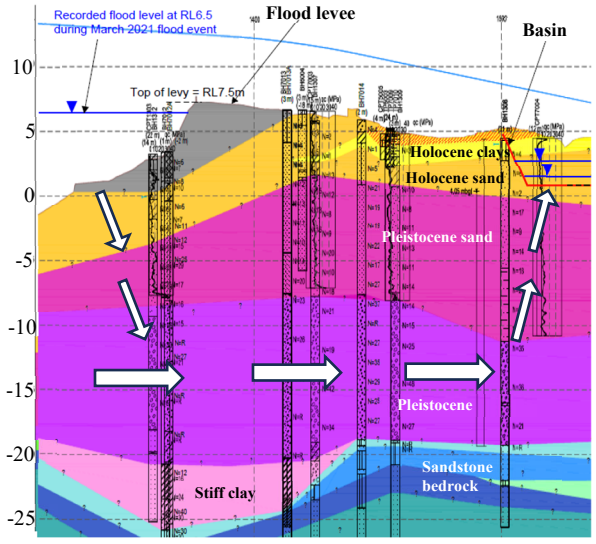

Figure 4. Typical long section and outline of the basin (exaggerated vertical scale)

6 PERMEABILITY OF ALLUVIAL SAND

Three different approaches have been adopted to estimate the permeability of the Holocene and Pleistocene sand layers, namely:

- In-situ slug tests;
- Laboratory constant head permeability tests; and
- Hazen's (1911) empirical correlation.

Particle size distribution (PSD) curves for sand samples at different depths are presented in Figure 5. Based on the PSD curves, the Holocene and Pleistocene sand can be classified as uniformly graded sand. Both sand units are similar in grading, i.e. fine to medium grained. Permeability of sands can be estimated using Hazen's formula (Eq. 1) which was developed for uniform sands:

$$\text{Permeability, } k \approx C\,(D_{10})^2 \quad \text{(m/sec)} \qquad (1)$$

where C is a correlation factor and D_{10} is the 10 per cent particle size in mm taken from the PSD curves. C could vary between about 0.007 and 0.014. By adopting a typical C=0.01, the estimated values are shown in Figure 6 together with the in-situ and laboratory permeability test results.

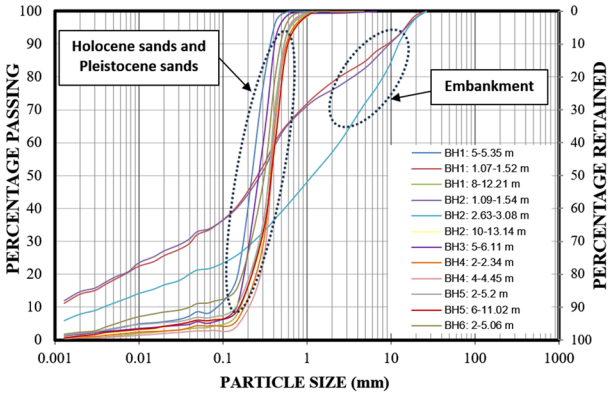

Figure 5. Particle size distribution of samples tested

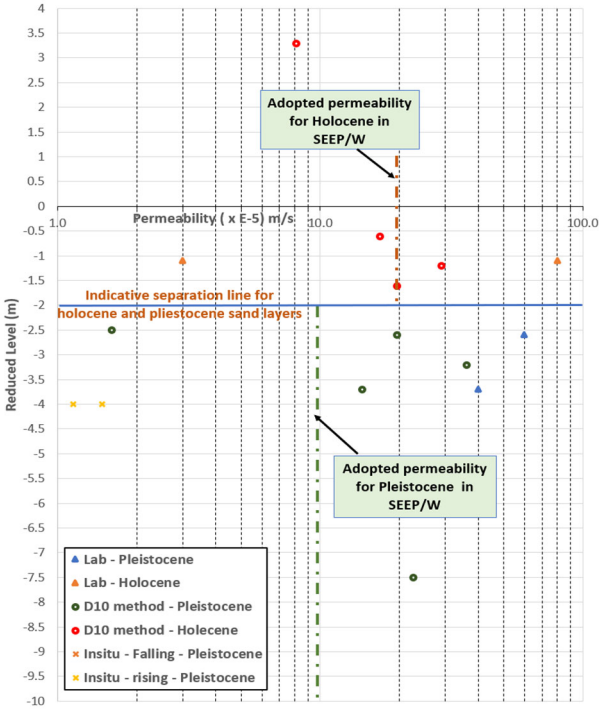

Figure 6. Estimated permeability of the sand layers

The two in-situ permeability (slug) tests were conducted immediately after borehole drilling and standpipes installation. Residual drilling mud within the sub-soil may have impeded water level recovery following slug removal or addition, leading to underestimated permeability values. Consequently, the permeability derived from the slug tests was likely much lower than the actual in-situ permeability. In contrast, laboratory constant-head tests indicate that the Holocene and Pleistocene sand layers possess significantly higher permeabilities than those suggested by the in-situ results. The higher laboratory values likely reflect the absence of drilling mud, reduced influence of in-situ stress, and the use of smaller, more uniform specimens, all of which can increase measured permeability compared with field slug tests.

7 BACK-ANAYSIS

2D Finite Element Analysis (FEA) has been carried out to assess the mechanism of groundwater flow leading to sand boiling at the basin using the commercially available software SEEP/W. A transient flow analysis has been performed to back-analyse the water level rise in the river and sand boiling in the basin with time. Details of the back-analysis and the assessment outcomes are discussed below.

7.1 *2D Hydrogeological Model*

A 2D section shown in Figure 8a capturing the relative distance between the river and the basin was adopted for the flow analysis. Figures 8b and 8c show the soil stratigraphy along the design section. Table 1 summarises the back-analysed hydrogeological properties of the soil layers. Figure 7 provides a comparative plot of hydraulic conductivity curves for the key layers in the model. No site-specific laboratory testing was undertaken to develop the hydraulic conductivity functions for the various soil layers. The hydraulic conductivity functions with matric suction were adopted based on the suggestion provided in SEEP/W for typical soils. However, without extensive testing, the hydraulic conductivity functions of the soils could not be confirmed or refined.

Note that a thin layer of sandy loam encountered at the basin floor has a relatively lower permeability than that of the underlying Holocene alluvium. The permeability contrast between the two layers was assessed to have contributed to sand boiling.

Table 1. Adopted hydraulic properties of key layers

	Typical thickness below basin (m)	Saturated Permeability (m/s)	Saturated water content (-)
Silty sand fill (sandy loam)	0.3	2e-7	0.4
Holocene sand	2.7	2e-4	0.35
Pleistocene sand	8.5	1e-4	0.3
Pleistocene gravel	9.5	1e-2	0.3

7.2 *Initial and Boundary conditions*

The initial groundwater level was set at RL 0.5 m, which was 0.5 m below basin floor and was also the initial river water level.

Figure 9 shows the rising of the monitored river water level with time during the 2021 flood event. This was applied as the boundary condition at the riverbed in the transient flow model as shown on the left side in Figure 8b.

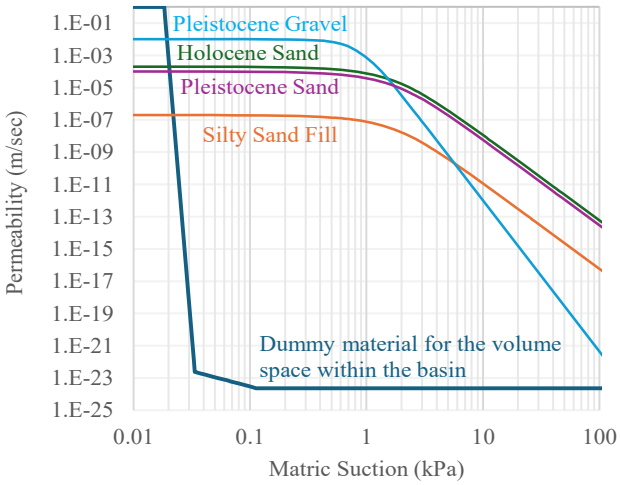

Figure 7. Hydraulic conductivity curves for key layers

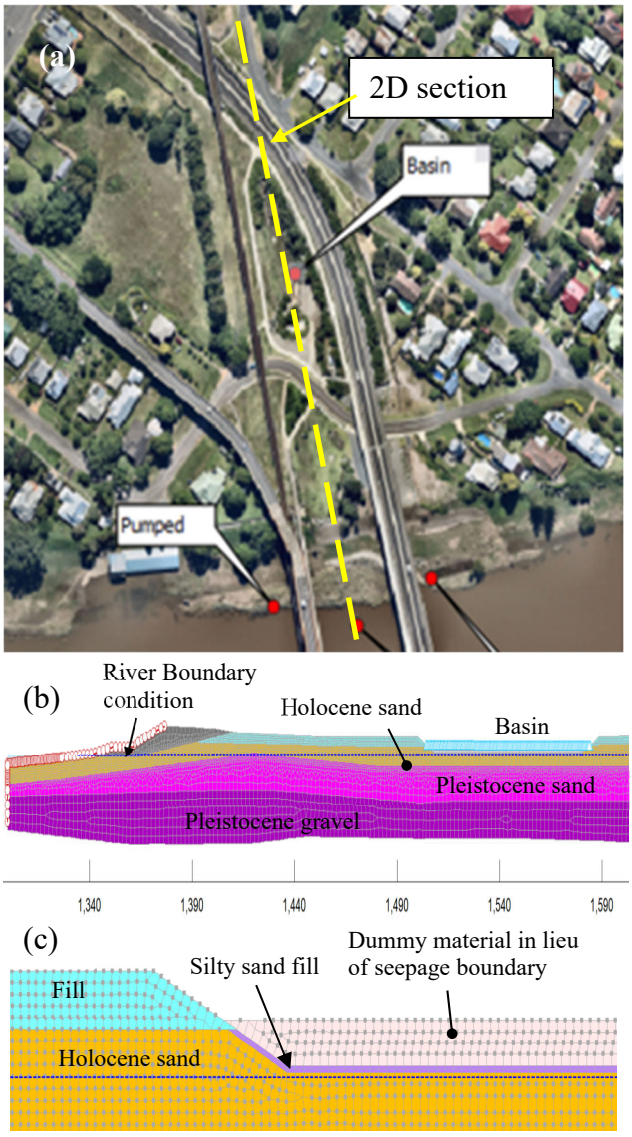

Figure 8. (a) 2D Section; (b) Overall hydrogeological profile; (c) Soil layers near the basin

Seepage groundwater is expected to enter the detention basin as the river water level increases. It is not appropriate to apply the potential seepage face boundary condition on the basin floor and batters as the seepage water that enters the basin will not be passed out of the domain and the pressure head will

not be equal to zero after the phreatic surface reaching these boundary nodes. An alternative way to model groundwater entering the basin was the adoption of a dummy material for the volume space within the basin with a hydraulic conductivity function as shown in Figure 8c and Figure 7 that has the following characteristics:

- High saturated conductivity of 1m/s
- Low air entry value of less than 0.05kPa
- Unsaturated conductivity of close to zero

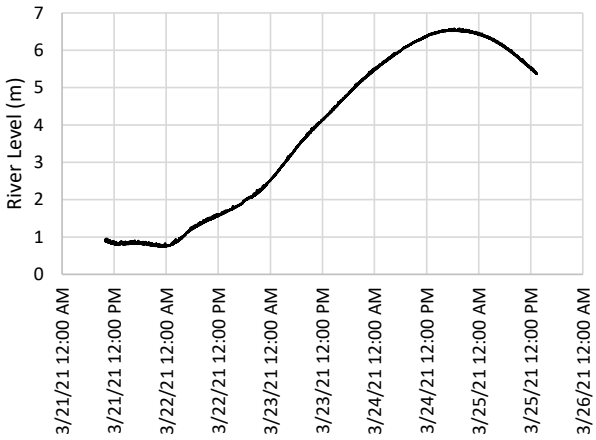

Figure 9. Monitored rising river water level with time

7.3 *Back-analysis findings*

The transient seepage flow analysis has indicated that as the river water level increases, groundwater flows towards the right boundary and the basin due to the hydraulic gradients created by the flooding in the river. In addition, the water flow is most prominent in the Pleistocene gravel because of the expected significantly higher permeability of gravel than the overlying sand units.

The preferential flow path has been assessed in seepage analysis as shown in Figure 10a and has also been shown diagrammatically in Figure 4. As the river water rose to RL 5.6 m (at approximately 5 am on 24 March per Figure 9), the groundwater was assessed to have entered the basin with a basin water level at RL 1.3 m (0.3 m above basin floor). Pore water pressure was assessed to have built up below the sandy loam layer at this point of time as it has a lower permeability than that of the underlying Holocene sand. For example, the assessed total stress at Point A (see Figure 10b) below the sandy loam was 11 kPa, which was lower than the assessed pore water pressure of 16 kPa. The assessed effective stress was -5 kPa, hence indicating the occurrence of sand boiling. As the basin water rose further to RL 2.4 m (1.4m above basin floor, see Figure 10c), it was assessed that sand boiling subsided as indicated by the positive effective stress at Point A (+2 kPa = total stress of 22 kPa – pore water pressure of 20 kPa). The assessed results outlined above are consistent with the observations outlined in Section 4.1.

The back-analysis also implies that the permeability of the Holocene sand is consistent with the estimated permeability values using the approaches discussed in Section 6 above. However, the back-analysed permeability of the underlying Pleistocene sand appears to be lower than those estimated from the laboratory permeability tests and Hazen's empirical correlation with particle size distribution.

8 REMEDIAL OPTIONS

Four remedial options were proposed to mitigate future sand boiling failure and slope instability as follows:

8.1 *Option 1 – Placement of rockfill*

The placement of rockfill on the basin floor is to increase the total stress that would counteract the uplift seepage pressure and to prevent the formation of sand boiling due to the loss of effective stress. Removal of the low permeability sandy loam at the basin floor followed by placing a nominal rockfill layer thickness of 1 m was proposed. A layer of filtration geotextile placed beneath the rockfill was also proposed to act as a filter to prevent sand migration into the basin.

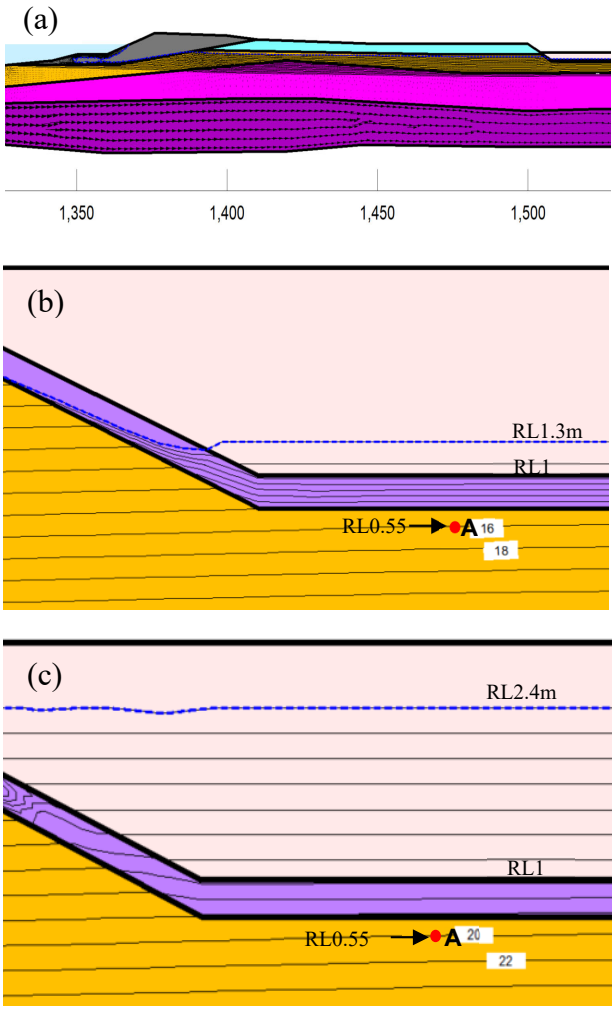

Figure 10. SEEP/W transient flow analysis results: (a) water flow vector, (b) pore water pressure contour with basin water level at RL 1.3m, and at (c) pore water pressure contour with basin water level at RL 2.4 m

8.2 *Option 2 – Installation of relief wells*

The installation of pressure relief wells can prevent sand boiling by reducing the uplift pressure beneath the basin floor to a value less than the submerged weight of the soil. The spacing and the depth of the relief-well system was to be designed to reduce the seepage pressure to a safe level.

8.3 *Option 3 – Mass soil mixing*

Migration of sand particles from the substrata to the floor of the basin occurs through the high permeability of the existing subsoil when the river is flooded. The reduction of the permeability of subsoil prevents the migration of fine particles by controlling the water movement. Mass soil mixing is a ground improvement technique that can reduce the permeability of the in-situ soil by mixing the existing soil with low

permeability binders while mechanically disaggregating the soils. The mixing process can also create a cemented zone such that the sand is bonded together.

8.4 *Option 4 – Installation of precast box culvert*

This option would include extending the existing box culvert and base slab between the existing northern box culvert and the pump station to accommodate the upstream water flow from within the town. The backfilling of rockfill along and above the culvert will counteract the uplift seepage pressure and prevent the formation of sand boiling due to the loss of effective stress.

8.5 *Final solution*

The adopted final solution was essentially Option 1 where invert of the basin was lined with 150 mm thick concrete over 1 m thick rockfill and high strength geotextile. The selection of this option was mainly based on aesthetic and public preference considerations.

The low permeability sandy loam at the basin floor was removed prior to placing the rockfill layer. The completed remedial work is shown in Figure 11.

Figure 11. View of the basin shortly after construction of the remedial works

9 CONCLUSIONS

Sand boiling and the associated internal backward erosion are typically recognized as one of the most important aspects in the design of hydraulic structures with relatively permeable foundation materials. However, this mechanism is usually not considered in the design of highway or railway projects.

This case study demonstrates that sand boiling and internal backward erosion can occur in detention basin close to rivers where the foundation materials comprise sands and gravels. For this case study, while the basin is some distance away from the river, the presence of the highly permeable gravel layer below the sand layers provides a relatively short drainage path for the water in the river to flow down to the gravel and then up towards the basin.

When the hydraulic gradient between the river level and the groundwater level under the basin became sufficiently high during river flood events, high seepage pressure below the basin floor was generated. With the presence of the low permeability sandy loam topsoil at the basin floor, effective stress below the topsoil layer became very low or even negative, causing heaving and blowing out of the basin floor. Sand boiling, ground subsidence and slope instability then followed.

The final remedial solution was to remove the low permeability sandy loam topsoil followed by placing a 1 m thick rockfill. A concrete strip was also placed at the invert of the basin. The objective of the solution was to ensure the total stress is always greater than the pore pressure and the hydraulic gradient below the basin will be reduced during future floods.

10 REFERENCES

Bezuijen, A., Vandenboer, K., van Beek, V. and Robbins, B., 2019. Pressure drop in vertical pipes of sand boils. In: *Proceedings of the XVII ECSMGE Geotechnical Engineering Foundation of the Future*, Reykjavik, Iceland, paper 154.

Brennan, A., 2008. Observations on sand boils from simple model tests. In: *Proceedings of the Geotechnical Earthquake Engineering and Soil Dynamics Congress IV*, Sacramento, California.

Hazen, A., 1911. Discussion of Dams on sand foundations. In: A.C. Koenig, ed. *Transactions of the American Society of Civil Engineers*, 73(3), pp.199–203.

Pabst, M., Engemoen, B., Hanneman, D., Redlinger, C. and Scott, G., 2008. Heave, uplift, and piping at the toe of embankment dams – A new perspective. In: *Proceedings of Dam Safety 2012*, ASDSO, Denver, CO.

Robbins, B.A., Stephens, I.J., van Beek, V.M., Koelewijn, A.R. and Bezuijen, A., 2020. Field measurements of sand boil hydraulics. *Geotechnique*, 70(2), pp.153–160.

Schaefer, J.A., O'Leary, T.M. and Robbins, B.A., 2017. Assessing the implications of sand boils for backward erosion piping risk. In: *Proceedings of Geo-Risk 2017*, GSP 285, Denver, Colorado, pp.124–136.

TAW, 1999. *Technical report on sand boils (piping)*. Delft, The Netherlands.

US Society on Dams, 2021. *Introduction to internal erosion in dams and their foundations*. USSD Embankment Dams Committee, USA.

Van Beek, V.M., de Bruijn, H.T.J., Knoeff, J.G., Bezuijen, A. and Förster, U., 2010. Levee failure due to piping: A full-scale experiment. In: *Proceedings of the International Conference on Scour and Erosion (ICSE-5)*, San Francisco, California.